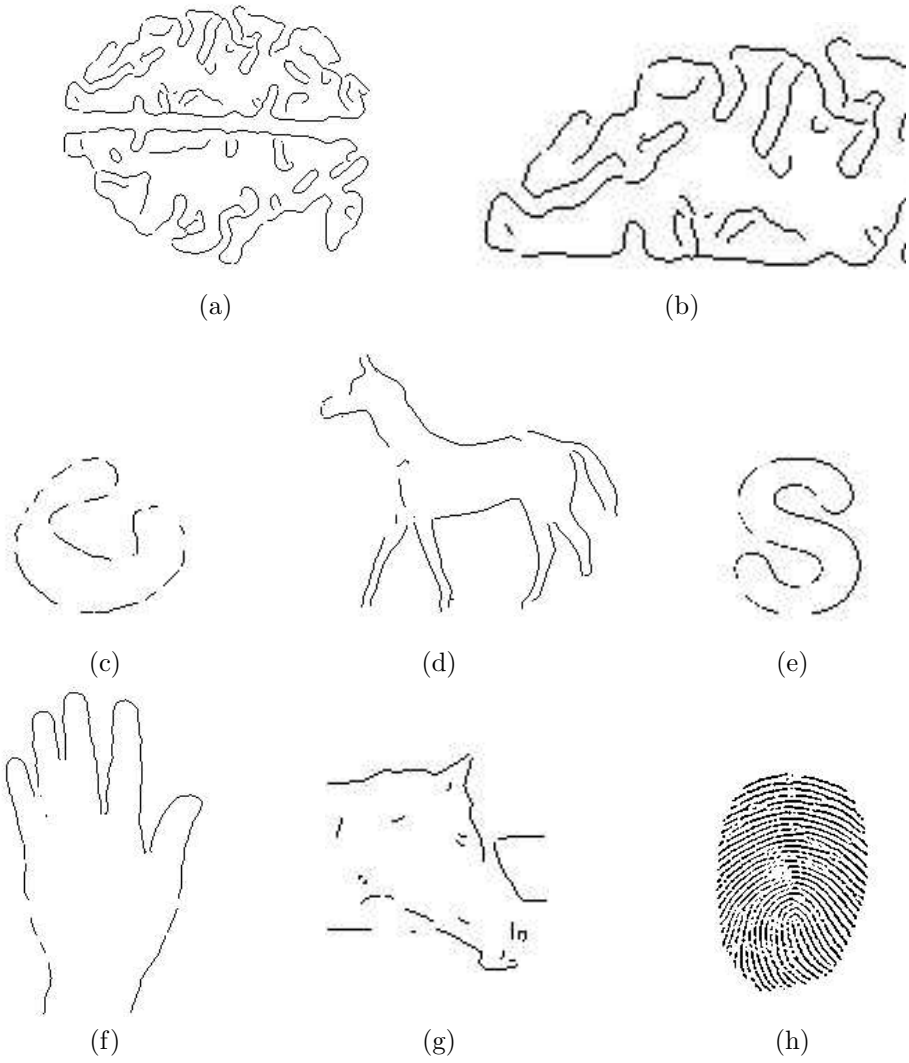

Figure 5.22: Uncompleted contours.

corrupted with gaussian noise (fig.5.20(a)) and a character 'S' with uniform noise added (fig.5.20(c)). Meanwhile the set of real images is displayed in fig.5.21.

The different image features used to select points (contours in fig.5.22) lying on the objects of interest are edges, ridges and gray level. We have chosen the following standard algorithms to compute them: Canny for edges, curvature for ridges and gray-level thresholding. To reduce the impact of noise and textured backgrounds, all images have been previously smoothed with a gaussian filter of $\sigma = 2$. For noisy images, contours correspond to edges of the smoothed images of fig.5.20(b), (d); for the

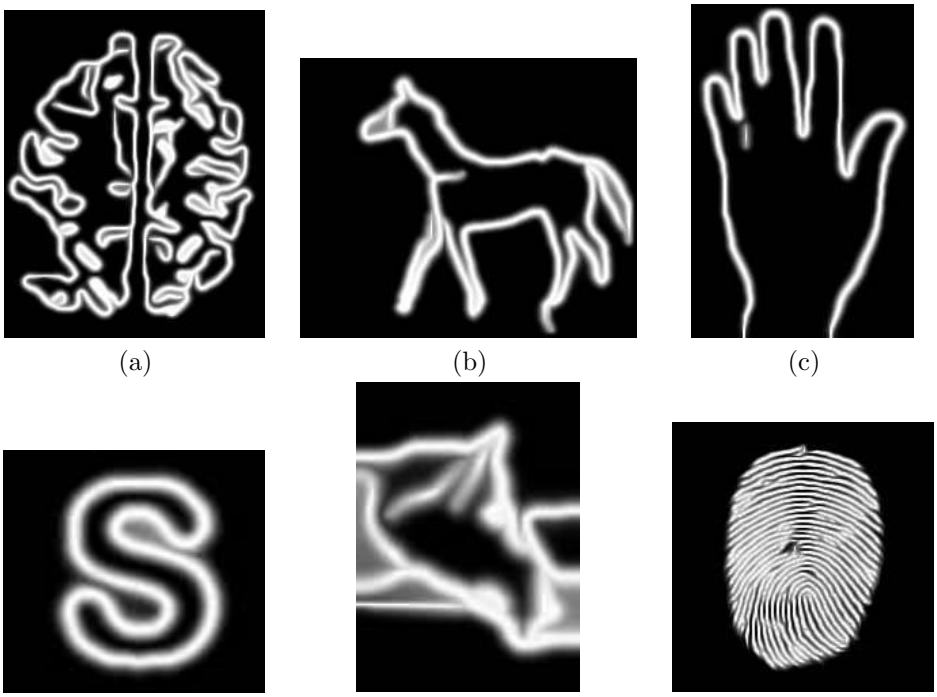

Figure 5.23: Extensions of brain (a), horse (b), hand (c), 'S' (d), head (e) and fingerprint (f).

real images of fig.5.21(a)-(e), we used edges in combination with pixel gray level in the brain image and for the fingerprint in fig.5.21(f), image ridges. The contours obtained, shown in fig.5.22, include cases deserving special care, such as corner restoration (horse ears in fig.5.22(d), (g) and finger joints in fig.5.22(f)) and dense lines prone to merge (fingerprint in fig.5.22(h)).

The numeric scheme used to compute solutions to (4.3) is an explicit Euler scheme for non-linear heat equations stabilize by means of the stop criterion critB given in Section 5.1.1. The parameters used in the computation of the coherence vector fields are an integration scale $\rho = 2$ and a regularization scale $\sigma = 0.5$. In the case of large gaps (fig.5.22 (e), (g)) vector fields are dynamically updated every 300 iterations. We have used the ridgeness measure described in [45] to compute the ridges of the extension that yield the curve closure and serve to update vector fields. According to the theoretic analysis given in Section 4.2.1, distance based vector fields properly recover a model of corners and linear fields avoid merging in the contours to complete. Therefore, for the sake of a maximum accuracy and reliability in the closed models, we have chosen the distance based DVF for restoration of contours in fig.5.22(a)-(h) and a linear LVF closing in the case of the fingerprint (fig.5.22(i)).

The final states achieved are the characteristic functions representing the recon-

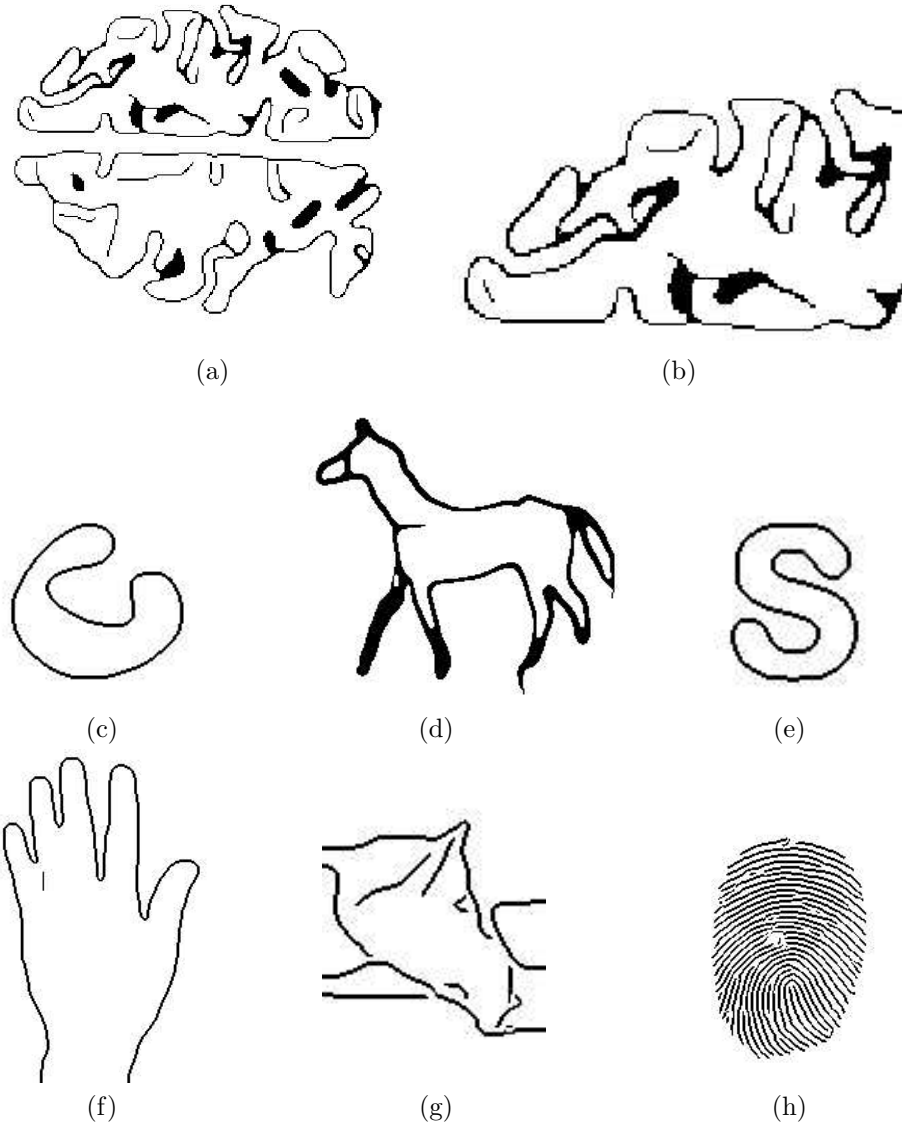

Figure 5.24: Reconstructed contours using DVF (a)-(g) and LVF (h).

structed shapes shown in fig.5.23 and their ridges yielding contour closures are displayed in fig.5.24. In the case of smooth contours, such as the noisy images (fig.5.20) and the hand (fig.5.21 (c)), ridges of the extensions are continuous lines that constitute accurate curve models (fig.5.24(c), (d), (f)). However, T-junctions produce discontinuous ridges so that reconstructions of the brain and horse (fig.5.24(a), (e))

were extracted via a morphological thinning of a thresholded version of the extensions.

Because it is based on the distance map to the open contours, closings achieved using DVF recover shape curvatures, such as the concave part of the non-convex contour in fig.5.24(c) and the character 'S' in fig.5.24(e). Besides it properly closes the acute angles of the horses ears (fig.5.24(d), (g)) and the hand finger joints (fig.5.24(f)). We may draw the reader attention towards the closures of the brain ridges, better appreciated in the detail of fig.5.24(b), for an example of DVF accuracy. Merging in the case of the horse ear and tail is a result of the way (thinning) contours are extracted. On the other hand, thanks to its linearity, LVF fingerprint closure does not merge line ends at the boundary and yields an accurate closure because of a small gap size without acute angulation.

5.3 Modelling Shapes with the Curvature Vector Flow

In this section we apply CVF to smooth shape representation with its application to object segmentation in combination with ACC. In order to assess the proposed segmenting strategy, two different experimental issues should be addressed. First, we will check accuracy of shape models attained with CVF, that is, its capability of adapting a snake to non-convex shapes. Second, quality in the segmentation of real images will be compared to results using geodesic snakes.

5.3.1 Shape Representation

Given a closed curve in the plane, a compact way of representing it is through an approach by means of a parametric B-spline snake. We recall the reader that a parametric snake [38] is a curve $\gamma(u) = (x(u), y(u))$ that minimizes the energy functional:

$$E(\gamma) = \int_{\gamma} (E_{int} + E_{ext}) du = \int_{\gamma} (\alpha ||\dot{\gamma}||^2 + \beta ||\ddot{\gamma}||^2 + E_{ext}) du \ ,$$

where the external energy depends on the image object to model and can be either a distance map or a function of the original image gradient. The parameters α and β determine the stiffness of the deformable model and are in the range $[0, 1]$. In any case the optimal curve is obtained by means of the Euler-Lagrange equations associated to E, which are equivalent to solving a linear system:

$$Ax = -\nabla E_{ext} \ .$$

The numeric iterative scheme is given by:

$$x_{t+1} = (A + \lambda I)^{-1} (\lambda x_t - \nabla E_{ext})$$

where I denotes the identity matrix, A the stiffness matrix [38] and λ is a viscosity parameter. An important remark is that stability of the finite difference scheme depends upon the viscosity parameter, which must be increased if α, β decrease. This viscosity parameter determines the speed of convergence, the higher it is, the

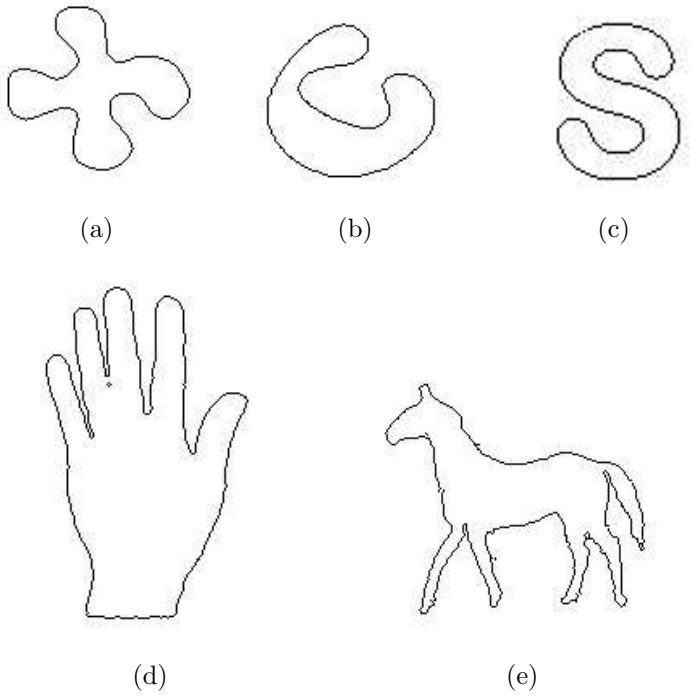

Figure 5.25: Set of test shapes: clover (a), highly non-convex curve (b), character 'S' (c), hand (d) and horse (e).

slower the snake converges. We consider the snake has reached its final state when its total energy stabilizes.

Experiments focus on the efficiency and accuracy of CVF when non-convex contours are modelled. Accuracy has been computed in terms of snake convergence, given by the snake maximum Euclidean distance to the original closed contours. Efficiency is given by the CPU-time the initial snake takes to reach its final state. Since the stop criterion is in terms of the stabilization of the external energy, the asymptotic behavior of the functional E is also a measure of the method efficiency. An oscillating graph for E hinders stopping the deformable model with the former stop criterion and the final snake must be obtained after a fixed number of iterations.

We have tested the external potentials for different values of the snake parameters, α and β, in order to check if the energies could support large values and still guarantee convergence of the snake to the curve of interest. As noticed before, supporting large values for α, β is also a signal of efficiency, since the larger these parameters are, the faster the snake converges. The snake has been initialized inside and outside the object of interest. We have compared CVF to the results obtained using a GVF-regularized gradient of the Euclidean distance map (DM) and GVF applied to the edge map.

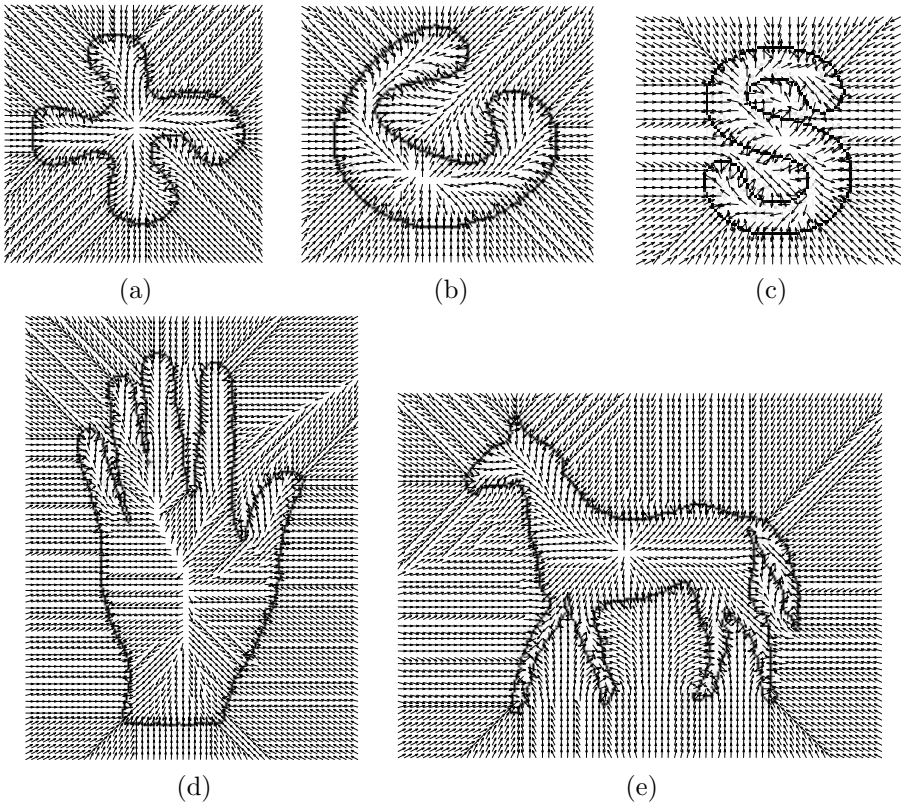

Figure 5.26: CVF on clover (a), highly non-convex curve (b), character 'S' (c), hand (d) and horse (e).

The shapes chosen are depicted in figure 5.25. The external force given by CVF is shown in figure 5.26. Convergence of snakes for the different external forces is shown in figure 5.29 and the final model obtained is depicted in figure 5.30.

In terms of an accurate model of the shape, CVF is the only external energy that adapts the deformable model to all curves, whatever position (inside or outside the object of interest) of the initial snake. The other two external energies fail to obtain an accurate model when the initial snake lies inside the object of interest. Convergence to the character 'S' and horse in fig. 5.29 and the final shapes of fig. 5.30 illustrate this bad-pose of the snake inner convergence with GVF and DM. In the case of the character 'S', saddle points of both GVF and DM, make the snake oscillate at closed shapes which fail to reach the extremal boundary of the 'S'. Irregularities in the gradient of the horse external energy, produces open final snakes (fig. 5.30(b),(c)) approaching only a part of the animal's contour. Notice the accuracy and smoothness of the final model of the horse achieved with CVF (last row of fig. 5.30(a)). In the case of an outer initial snake, GVF succeeds in adapting to non convex shapes such that the angle θ does not turn more that π between two consecutive inflexion points

(like the clover of fig. 5.30(b)). However the snake gets trapped at the saddle points that highly non convex shapes (second row of fig. 5.30(b)) produce in the vector field. The external force field obtained by a regularization of the gradient of DM using GVF is the worst performer. Even for small values of α and β, the external force is not strong enough to attract the snake to non-convex shapes, even in the case of shapes (like the clover of fig. 5.30(c)) with the angle θ turning less than π between two consecutive inflexion points. Figure 5.27 summarizes these results in the form of maximum Euclidean distance to the contour of interest versus number of iterations. Notice significant differences of the maximum distance between CVF and DM/GVF in the case of convergence to highly non-convex shapes (fig. 5.27 (a),(c)).

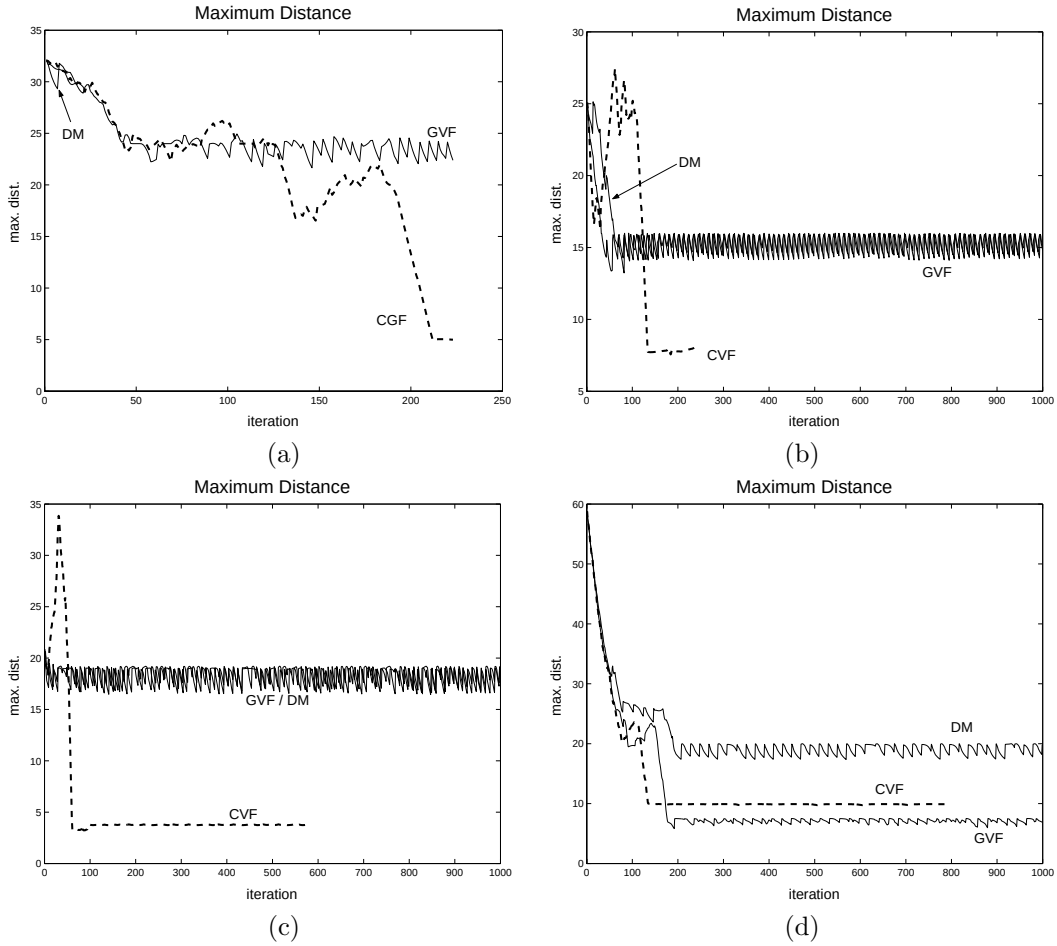

Figure 5.27: Snake accuracy, interior convergence for highly non convex shape (a) and the clover (b) and the corresponding exterior convergence (c) and (d)

Concerning efficiency, CVF is, again the best performer, since attains accurate

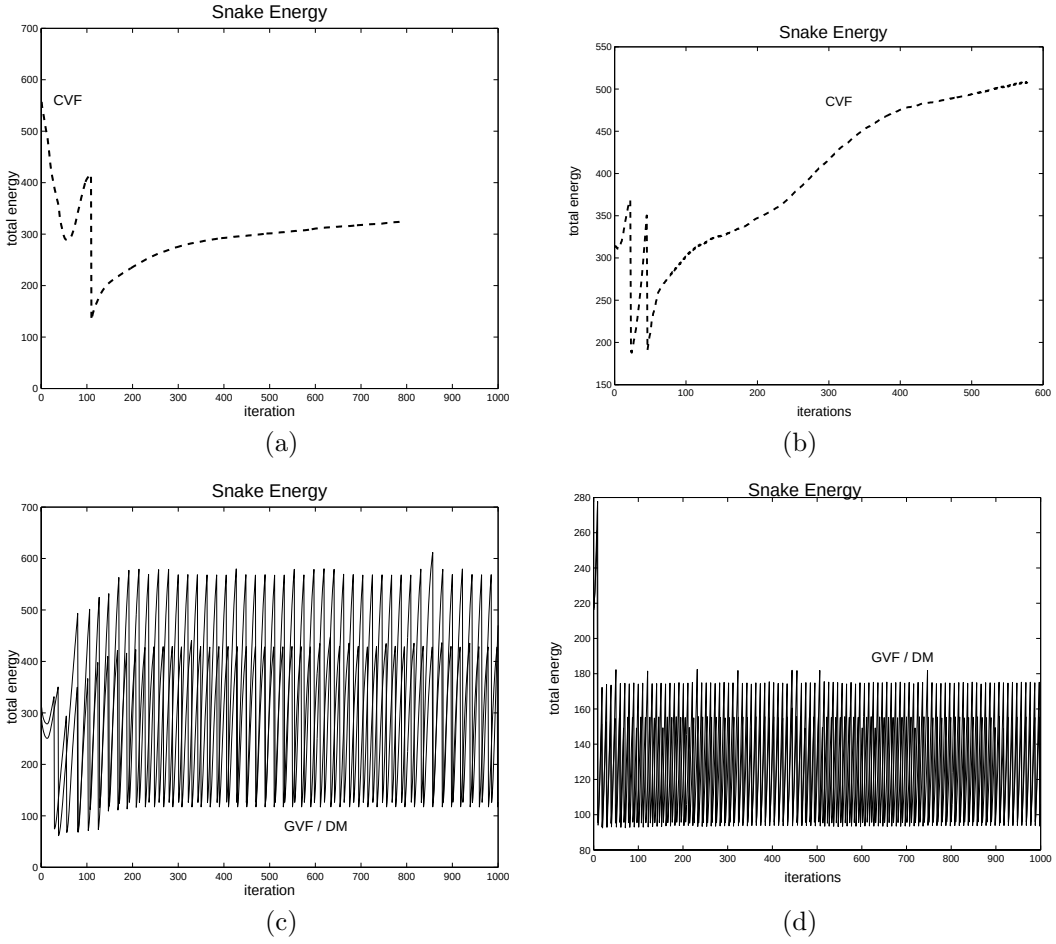

Figure 5.28: Evolution of snake energy, CVF exterior convergence for highly non-convex shape (a), the clover (b) and the corresponding GVF/DM convergence (c) and (d)

models in optimal time, meanwhile GVF is the worst of the methods. Times for DM have not been taken into account since the method does not produce good enough segmentations as to be taken into account. The main reason for this difference in times lies on the fact that, due to the smoothness of the map, deformable models guided by CVF do not need, in general to be re sampled during evolution. On the other side, since GVF does not take into account the geometry of shapes, the snake sampling must be refined at points where two opposite directions compete (that is when entering into concave regions) in order to guarantee convergence to a closed contour. This increases the computational time of GVF up to four times CVF time in the case of the hand or the horse. Also in terms of the stiffness parameters, α

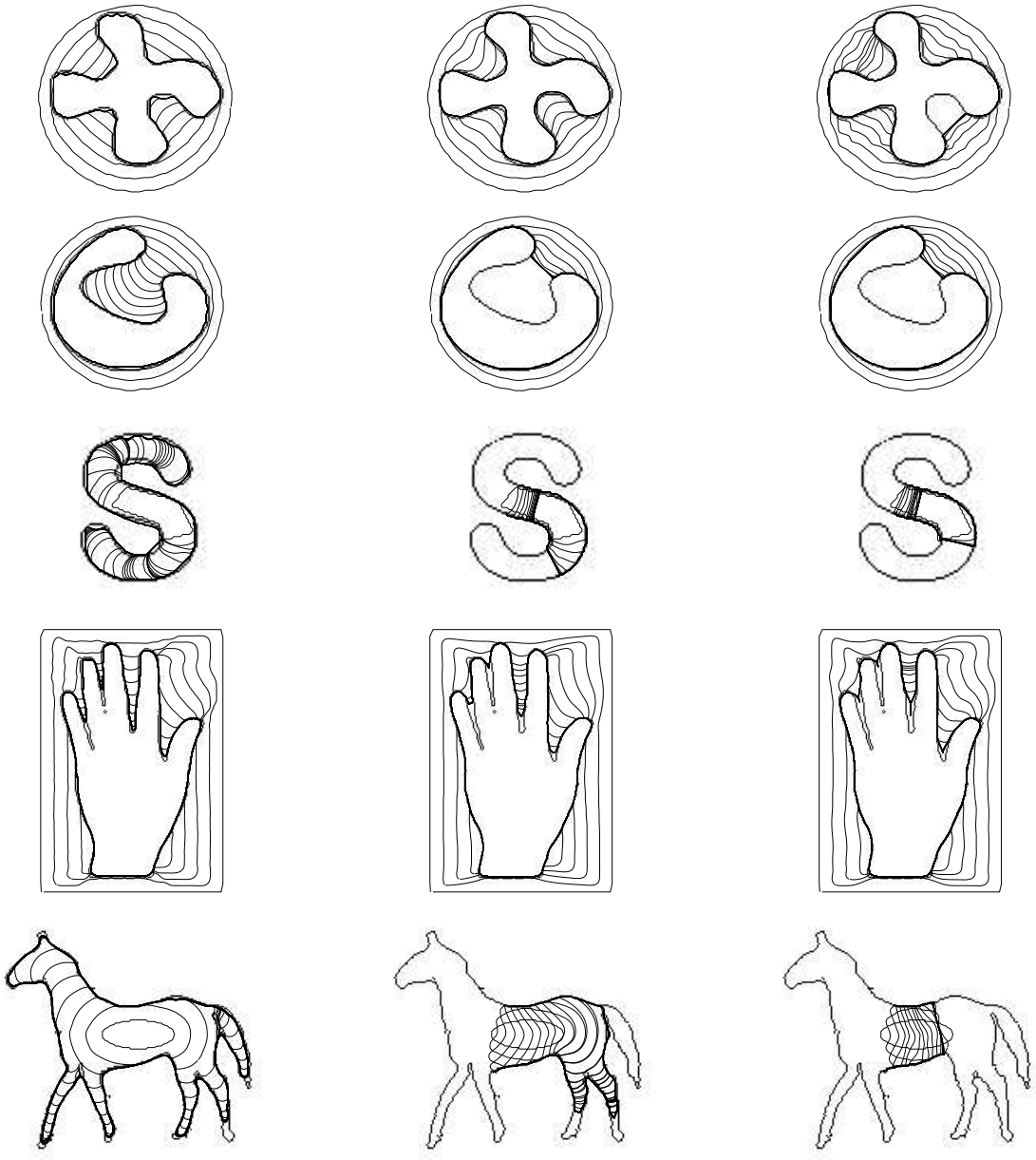

(a) (b) (c)

Figure 5.29: Snake convergence, CVF (a), GVF (b) and regularized DM (c).

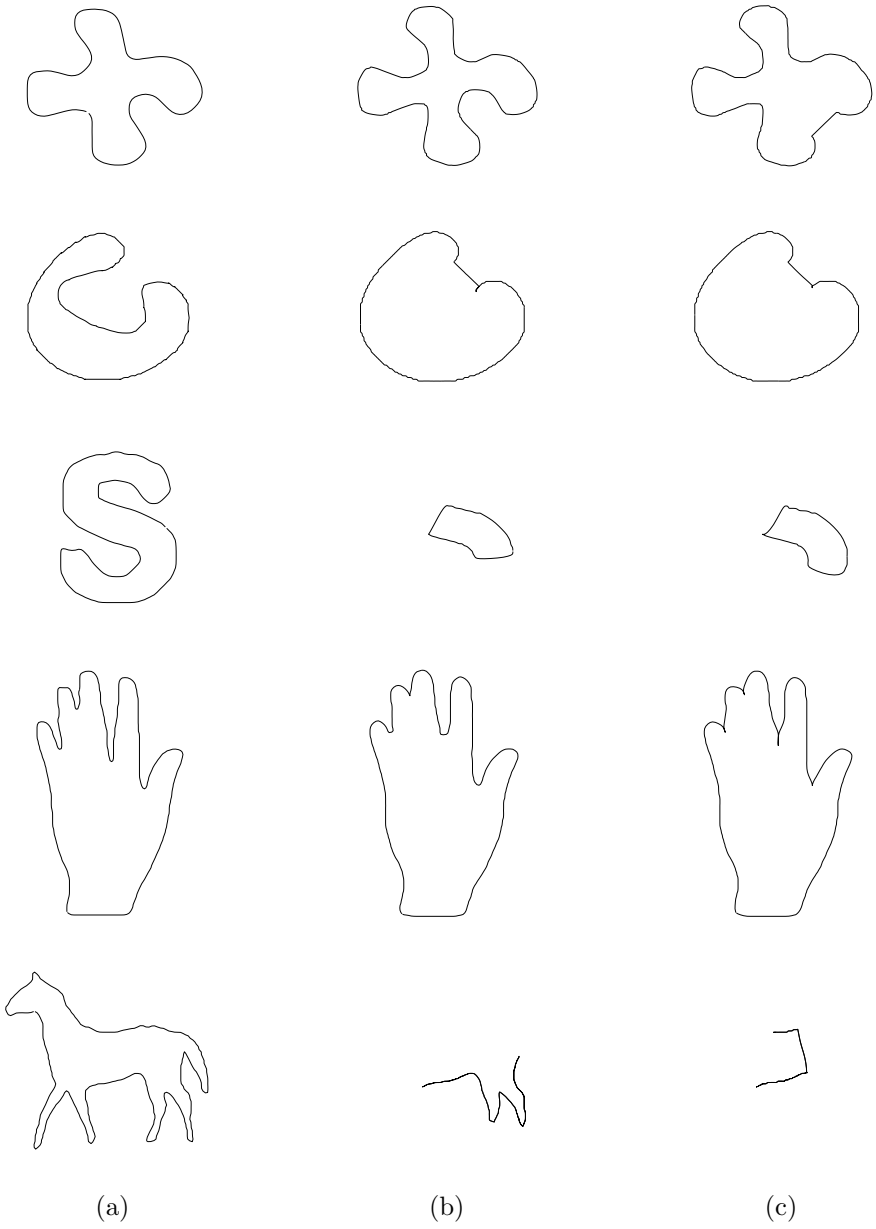

Figure 5.30: Shapes obtained with CVF (a), GVF (b) and regularized DM (c).

and β, CVF is the most efficient. Our tests done for different values of the stiffness parameters show that CVF supports, in general, values in the whole range of $[0, 1]$. Only in extreme cases like inner convergence to the horse and outer convergence to

the hand, α and β must be smaller than 0.3 if we want a reliable final model.

Another issue worth to be considered is the asymptotic behavior of the snake convergence. Figure 5.28 shows the evolution of the snake energy in time for convergence to the clover and the highly non-convex shape of fig. 5.29, in the case of a CVF guided snake (fig. 5.28(a),(b)) and a DM/GVF one (fig. 5.28(c),(d)). Notice that deformations under CVF present a smoother asymptotic behavior, compared to the highly oscillating graphics of DM and GVF. This oscillating behavior strengths when the snake gets trapped at saddle points. A smooth energy implies a strong advantage since a stop criterion in terms of the snake total energy is a robust way of determining the final state for CVF guided snakes.

5.3.2 Application to Object Segmentation

Smooth shape representation plays an important role in image segmentation. Connecting a set of points that lie on the object of interest, whatever its geometry, is still an open question. Parametric snakes [38] and geodesic snakes [11], [12] are the two techniques most commonly used by the image processing community. On one hand, in spite of yielding smooth models, poor convergence to concave shapes limits classic snakes applicability. On the other hand, geodesic snakes convergence to multiple objects, does not compensate for their slow convergence to piece wise linear curves that may have penetrated into large gaps of contours. We argue that the framework of classic snakes provides with an efficient way of shape modelling, both in terms of computational time and compact representation of a reliable model of the shape. The segmenting strategy we propose is the following.

We base image object segmentation on the approximation of a set of (possibly unconnected) points that conform to given characteristics exclusive to the contour of the object we want to model. We consider that the object is successfully segmented once we have a closed contour approaching this set of points. We propose the following strategy to model uncompleted contours. First, we will apply functional extension using ACC to the selected set of points in order to produce a closed contour. Ridges of the final extension are the curve of level zero of the Curvature Distance Map (CDM) that serves to compute the Curvature Vector Flow that will guide a parametric B-spline snake to a model of this contour.

We devote the last experiment to efficiency and accuracy of the former segmenting strategy compared to geodesic snakes. The set of images are the noisy images of fig.5.20 and the real images of fig.5.21 (a)-(c) in Section 5.2. Completions of the extracted contours (see fig.5.22) given by ACC (see fig.5.31) are the input zero level set for the computation of CVF. For geodesic snakes, we have used their original formulation [12] for image edge-based segmentation:

$$\gamma_t = (g(|\nabla I|)(c + \kappa) - \langle \nabla g(|\nabla I|), \overrightarrow{n} \rangle) \overrightarrow{n}$$

where $g(|\nabla I|) = 1/(1 + |\nabla I_\sigma|^2)$ and c is the area constrain constant. The function g has been computed over original images (fig.5.21 (a), (c)) in the case of the brain and the hand, and the filtered image of fig.5.20(b) for the noisy non convex shape. For a better comparison to our strategy and to reduce noise impact, the edge measure g

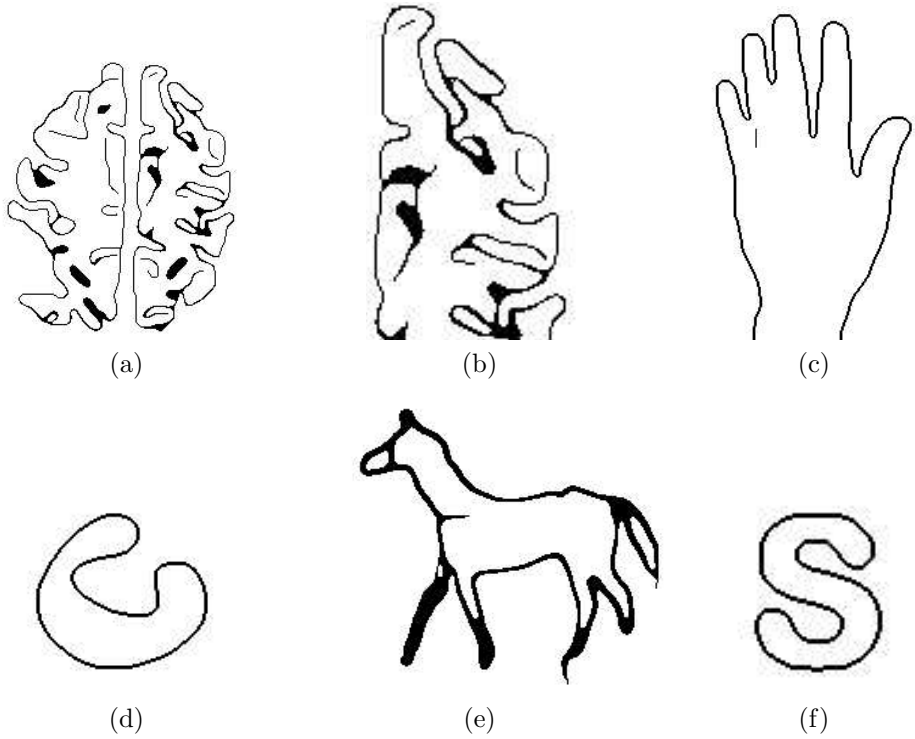

Figure 5.31: Reconstructed contours using DCV.

is computed over the image contours of 5.22 in the case of the character 's' and the horse.

Both in the case of geodesic and parametric snakes, we consider the snake has reached its final state when its total energy stabilizes. Snake convergence is illustrated in fig.5.32 and fig.5.33 (with yellow curves representing final geodesic snake segmentation). Segmentation using geodesic snakes strongly depends on the quality of image edges which makes their convergence to concave regions significantly decrease in the presence of noise (fig.5.32(b)) or highly non convex uncompleted contours. In noisy images, the regularization scale used to compute $|\nabla u_\sigma|$ must be increased to ensure a stable snake evolution. In the case of large gaps, the regularization scale must ensure that the gradient of g will close them, otherwise the snake could converge to an unconnected curve. However, the bigger the gaussian kernel is, the more prone to develop saddle points and ridges the image gradient is. Just to mention it, this phenomena still produces even if a regularization with GVF [**?**] is used. Since the constant c must keep within the range of $|\nabla g|$ if we want the snake to stop at image contours, we have that the area constraint term does not compensate ∇g bad behavior. Only in the case of noise free, non textured backgrounds (fig.5.33(d), (f)) geodesic snakes successfully adapt to contours.

On the other hand, segmentation using CVF only relies on the accuracy of the

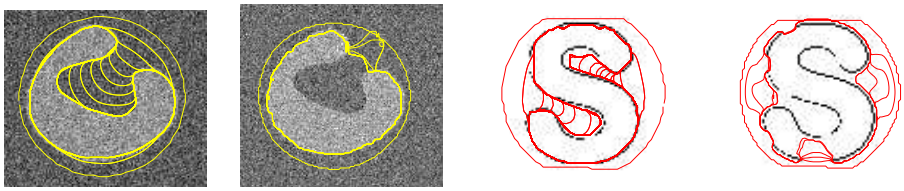

(a) (b) (c) (d)

Figure 5.32: Convergence to non convex shape using CVF snakes (a) and geodesic snakes (b). Convergence to character 'S' using CVF snakes (c) and geodesic snakes (d).

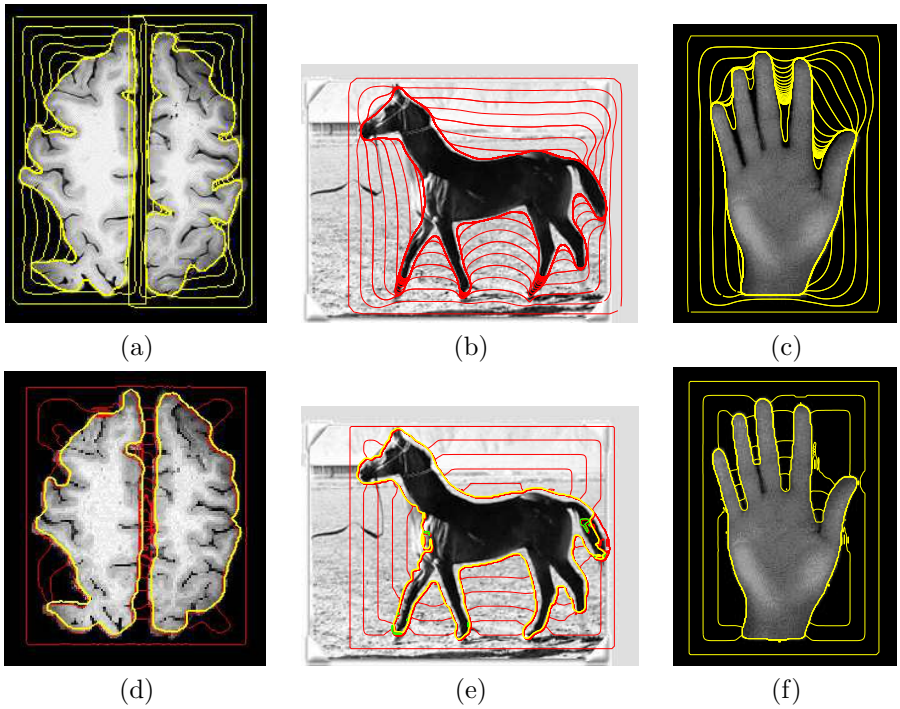

(a) (b) (c)

(d) (e) (f)

Figure 5.33: Snake Convergence to brain, horse and hand of CVF snakes (first row) and geodesic snakes (second row).

closed models yield by DVF, as CVF guarantees snake convergence to the zero level curve. Since the impact of noise was suppressed from the uncompleted contours of fig.5.22(d), (f), performance of our CVF parametric snake in noisy images (fig.5.32(a), (c)) clearly surpasses that of geodesic snakes. Also in the case of the horse, we obtain a more accurate representation, since the curve that geodesic snakes yield (fig.5.33(e)) has several connected components. Concerning unpolluted backgrounds (fig.5.33(a),

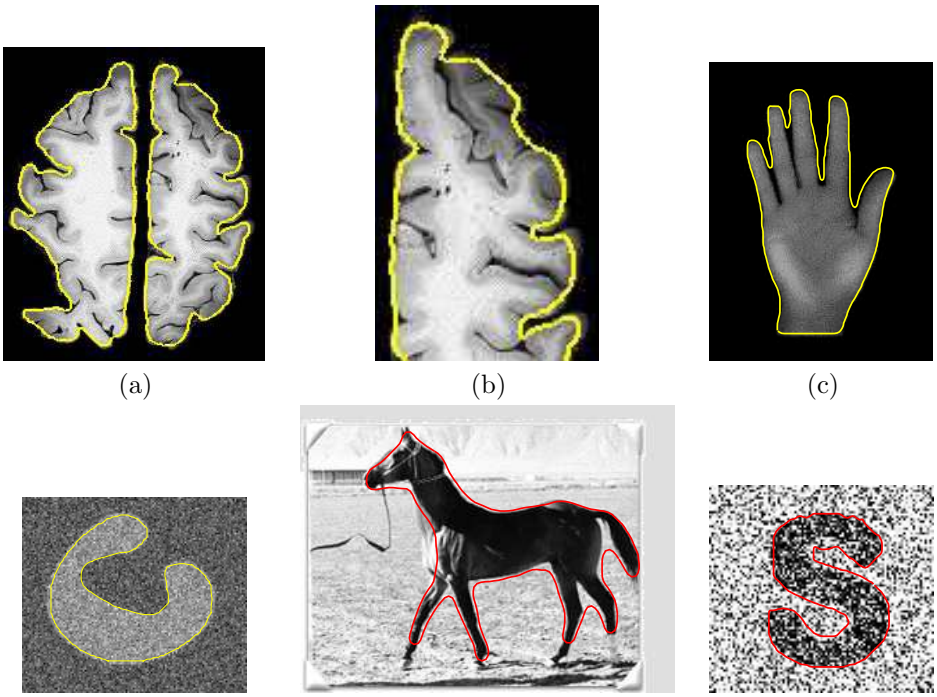

Figure 5.34: Segmentation using DVF/CVF.

(c)), the model of the brain (fig.5.34(a)) yielded by CVF is more precise than segmentation using geodesic snakes (fig.5.33(d)). Thanks to the accuracy of the brain closure (fig.5.24(a), (b)), the CVF contour captures more creases (fig.5.34(b)) than the geodesic model. Only in the case of sharp concave corners (hand of fig.5.33(d)) geodesic snakes perform better than CVF snakes. However, convergence to the hand (fig.5.33(c)) still compares to results obtain by geodesic snakes. Besides, final segmentations using CVF (fig.5.34), are, in all cases, smooth close models that conform to the original objects and keep their essential geometry. In order to increase accuracy, the final state achieved with CVF can be used as initial snake for a classic parametric snake.

Conclusions and Future Research

This work has shown that a geometric approach to PDE's enables designing image operators satisfying automatic stabilization at meaningful states smoothly approximating original objects. In particular, we have focused on shape modelling with segmenting purposes and a novel filtering technique(RCF), a contour closing algorithm (ACC) and an external snake potential (CVF) have been introduced.

The regularized curvature flow adds a measure of shape regularity to the mean curvature flow that prevents its degeneracy to a round point. Because the measure of regularity decreases over RCF orbits, the flow converges to a smooth model of the original shape. The image filtering defined by RCF level sets implicit formulation performs better than current filtering techniques as it achieves the best compromise between image quality and stabilization of the iterative numeric scheme.

Based on the grounds that a distance map represents the evolution of an initial curve in time under a geometric flow, CVF tracks evolution by mean curvature flow to avoid shocks. The gradient of this map is a smooth external force that guides in a natural manner the snake to the shape of interest. The fact that the force field takes into account the geometry of the final curve, makes convergence robust whatever the concavity of this curve is. Smoothness of snake evolution under CVF guarantees a robust convergence to smooth compact models of closed objects by means of a B-spline parametric snake.

Because the only requirement for computation of CVF is having closed contours, a novel approach to contour closing has been introduced. We have developed an implicit level sets formulation of a heat-like equation on manifolds in terms of a restricted diffusion operator. Such operators are an ideal tool for completion of contours regarded as a particular case of functional extension. Because ACC restricts diffusion to some curves of the image domain, the algorithm converges to closed models of shapes, as far as it a vector field representing the tangent of the contours to be closed. We propose a fat way of computing vector extensions (Coherence Vector Fields) conforming with tangents of unconnected contours at gap boundaries by applying Structure Tensor over either the contours masks or distance maps.

Finally, we have shown that a combination of ACC and CVF yields a segmenting strategy that compares and even surpasses performance of balloon-like geodesic snakes.

The theoretical setting developed suggests the following further research issues:

Future Lines of Research

1. **Applying restricted diffusion to a corner-preserving image filtering**

   By its own definition, a coherent vector field computed on the image yields smooth completions of the image significant curves, such as edges or ridges, that preserve curvature maxima. It follows that the associated restricted diffusion would uniformize their gray level while preserving their corners and smoothing noisy areas.

2. **Spline approximation of shapes with a given error**

   An efficient multiresolution approximation of curves with splines is still an open question. The first step is determine the minimum number of control points needed to obtain an approximate model of a curve with a given error. The CVF external force is the ideal starting point as it ensures snake convergence to closed shapes.

3. **Topological equivalence of analytic convexity conditions**

   The natural further research of the geometric equivalent of functional convexity is to give topological criteria in terms of the number of connected components (Morse theory [51]) of the functional level sets. Such simple criterion is the natural way of detecting inflexion points in GVF-like flows and provides a way of redefining the vector fields to ensure snake convergence for image segmentation.

4. **First order approximation of non-linear operators**

   Poor efficiency of numeric iterative processes mars performance of non-linear diffusion and hinders their design. Successive convolution with the kernel associated to their linear approximation would yield a first order fast accurate approach in the case of convergent operators.

5. **Apply all techniques (the developed and the forthcoming) to every single image available to find out their true applicability to the real world**

   An exhaustive validation of the techniques developed is a compulsory step for their reliable application to real problems.

Bibliography

[1] L.Alvarez, F.Guichart, P.L.Lions,J.M.Morel, *Axioms and Fundamental Equations of Image Processing*. Arch.Ration. Mech. and Anal.,123,199-257, 1993.

[2] G. Aubert, M. Barlaud,L. Blanc-Feraud, P. Chatbonnier. Deterministic edge-preserving regularization in computer imaging. *IEE Trans. Imag. Process.*, vol 6(2), Feb. 1997.

[3] Idan Bar-Sade and Avi Itzhaki. *Image Contour Extraction*. Tech. Report. TECHNION - The Vision Research and Image Science Laboratory.

[4] C.Ballester, M.Bertalmo, V.Caselles, G.Sapiro and J.Verdera. *Filling-In by Joint Interpolation of Vector Fields and Gray Levels* IEEE Trans. Image Processing, August 2001.

[5] J.Bigun, G.Granlund, J.Wiklund. *Multidiemnsional orientation estimation with applications to texture analyis and optical flow*. PAMI, vol. 13, 1991.

[6] J.Canny. *A Computational Approach to Edge Detection*, PAMI, vol. 8, 1986.

[7] F.Catté, P-L.Lions, J.-M.Morel, T.Coll. *Image selective smoothing and edge detection by nonlinear image diffusion*, SIAM J. Num. Ana., vvol. 29, 182-193, 1992.

[8] C.Cañero, P.Radeva. *Vesselness Enhancement Diffusion*, Patt. Recog. Letters 24 (2003), 3141-3151.

[9] R. Carmona, S. Zhong. *Adaptative Smoothing respecting Feature Directions* , IEEE Trans. Image Proc., vol. 7(3), March 1998.

[10] V.Caselles, F.Catté, T. Coll, F. Dibos, *A geometric model for active contours*. Numerische Mathematik, 66, pg.1-31, 1993.

[11] V. Caselles, B. Coll, J. Morel. *Topographic Maps and Local Contrast changes in Natural Images*, Int. J. Comp. Vision, vol 33, 1999.

[12] V.Caselles, R.Kimmel, G. Sapiro *Geodesic Active Contours*. Int. J. Comp. Vision.

[13] T. Chan, J. Shen. *Non-texture inpaitings by Curvature Driven Diffusions*. J. Visual Communication and Image Representation, 12(4), pp. 436-449, 2001.

[14] T. Chan, SH. Kang, and J. Shen. *Euler's elastica and curvature based inpaintings*, SIAM J. Appl. Math., 63(2), 2002.

[15] Y.G. Chen, Y. Giga, S. Goto, *Uniqueness and existence of viscosity solutions of generalized mean curvature flow equations*. J. Differential Geometry 33, pg. 749-786, 1991.

[16] L. D. Cohen. *On active contour models and ballons*. CVGIP:Image understanding, 53(2):211-218, 1991.

[17] L.D. Cohen, R. Kimmel, *Global minimum for active contour models: A minimal path approach*. Int. Journal Comp. Vision, 24 (1), pp. 57-78, Aug. 1997.

[18] S.D. Conte, C. de Coor. *Elementary numerical analysis, an algorithmic approach*. McGraw-Hill, NY, 1972.

[19] M.G. Crandall, H. Ishii, P.L. Lions *User's guide to viscosity solutions of second order partial differential equations*. Bulletin of the American Math. Society, 27, pg. 1-67, 1992.

[20] M.G. Crandall, H. Ishii, P.L. Lions *User's guide to viscosity solutions of second order partial differential equations*. Bulletin of the American Math. society, 27, pg. 1-67, 1992.

[21] E.B. Davies. *Heat Kernels and Spectral Theory*. Cambridge Tracts. in Math. 92, Cambridge University Press, 1989.

[22] Yu.V.Egorov, M.A.Shubin. *Partial Differential Equations I*. Enciclopaedia of Math. Sciences, vol.30, Springer-Verlag.

[23] L.C. Evans. *Partial Differential Equations*. Berkeley Math. Lect. Notes, vol.3B, 1993.

[24] D.Gil, P.Radeva. *Regularized Curvature Flow*. Computer Vision Center Tech. Report n 63, 2002.

[25] D.Gil, P.Radeva, F. Mauri. *IVUS Segmenation via a Regularized Curvature Flow*. Proceedings of CASEIB'02.

[26] D.Gil, P.Radeva, F.Vilario. *Anisotropic Contour Completion*, ICIP'03.

[27] D.Gil, P.Radeva. *Curvature Vector Flow to Assure Convergent Deformable Models*. EMMCVP'03.

[28] R.C.Gonzalez, P.Wintz. *Digital Image Processing*, Addison Wesley, Reading, MA.

[29] C.L.Epstein, M.Gage, *The Curve Shortening Flow in Wave Motion: Theory, Modeling and Computation*, A.Chorin and A.Majda, eds., springer-Verlag, New York, 1987.

[30] William H. Press, Brian P. Flannery, Saul A. Teukolsky, William T. Vetterling. *Numerical Recipes in C : The Art of Scientific Computing*. Cambridge University Press, 1993.

[31] D.R. Forsey, R.H. Bartels. *Surface Fitting with Hierarchical Splines*, Computer Graphics, April 1995.

[32] M.A.Grayson. *The heat equation shrinks embedded plane curves to round points*. J. Differential Geometry, Vol. 26, pp. 285-314, 1986.

[33] M.Gage, R.S.Hamilton. *The heat equation shrinking convex plane curves*. J. Differential Geometry, Vol. 23, pp. 69-96, 1986.

[34] M. Gage. *Curve shortening makes convex curves circular*. Invent. Math, vol 76, pp. 357-364, 1984.

[35] H. Hoppe, T. DeRose, T. Duchamp, M. Halstead, H. Jin, J. McDonald, J. Scheweitzer, and W. Stuetzle, *Piecewise smooth surface reconstruction*, Proc. ACM SIGGRAPH, pp. 295-302, July 1994.

[36] B. Jähne, *Spatio-temporal image processing*. Lecture Notes in Comp. Science, vol. 751, Springer, Berlin, 1993.

[37] G. Kanizsa, *Organization in Vision: Essays in Gestalt Continuation*. New York: Praeger, 1979.

[38] M.Kass, A.Witkin and D.Terzopoulos, *Snakes: Active Contour Models*, Int. Journal of Computer Vision, vol. 1, pp. 321-331, 1987.

[39] B. Kimia, K. Siddiqi, *Geometric Heat Equation and non linear Diffusion of Shapes and Images*. IEEE Proc. of Comp. Vision and Pattern Recognition, June 1994.

[40] B.Kimmia, A.Tanenbaum, S.W. Zucker. *On the Evolution of Curves via a Function of Curvature I:the Classical Case*. J. Math. Analysis and Aplications, vol 163, pp 438-458, 1992.

[41] B. Kimia, A. Tanenbaum, S.W. Zucker. *Toward a computational theory of shape: an overwiew*, Lecture Notes in Comp. Sci., vol 427, pp 402-407, Springer-Verlag, New York-Berlin.

[42] Ch. Knoll, M. Alcaiz, V. Grau, C. Montserrat, M.C. Juan, *Outlining of the prostate using snakes with shapes restrictions based on the wavelet transform*. Pattern Recognition, 32, pp. 1767-1781, 1999.

[43] P. Kornprobst, R. Deriche G. Aubert, *Nonlinear Operators in Image Restoration*, C.V.P.R, Porto Rico, june 1997.

[44] S.Lang *Linear Algebra*. Addison Wesley.

[45] Antonio M. López, David Lloret, Joan Serrat and JuanJ. Villanueva. *Multilocal Creaseness Based on the Level-Set Extrinsic Curvature* Comp. Vision Ima. Understanding vol. 77, pp. 111-144, 2000.

[46] Lysaker, Osher, Thai. *Noise Removal Using Smoothed Normals and surface Fitting*. UCLA, Applied Math. CAM-report-03-03.

[47] T. McInerney and D. Terzopoulos. *Deformable models in medical images analysis: a survey*. Medical Image Analysis, 1(2):91-108, 1996.

[48] R.Malladi, J.A.Sethian and B.C.Vemuri. *Shape Modeling with Front Propagation:A Level Set Approach PAMI*, vol. 17 (2), pp. 158-175, Feb.1995

[49] R.Malladi, J.A.Sethian. *Image Processing: Flows under min-max curvature and mean curvature*. Graphical Models and Image Processing, vol. 58 (2), pp. 127-141, Mar. 1996.

[50] S. Masnou, J.M. Morel, *Level Lines Based Discclusion*, Proc. IEEE Int. Conf. on Image Processing, Chicago IL, pp. 259-263, 1998.

[51] J.Milnor, *Morse Theory*, Annals of Math. Studies n 51, Princetown Univ. Press.

[52] P. Monasse, F. Guichard. *Fast computation of contrast invariant image representation*, IEEE Trans. Image Proc., vol. 9, 2000.

[53] J. Monteil, Azeddine Beghdadi, *A new interpretation an improvement of the Nonlinear anisotropic Diffusion for Image Enhancement*. IEEE Trans. IP, vol 21, n 9, Sep. 1999.

[54] D. Mumford, *Algebraic Geometry and its Applications*, Springer-Verlag, New York, 1994.

[55] M. Nitzberg, D. Mumford, T. Shiota, *Filtering, Segmentation and Depth*. Springer-Verlag, Berlin, 1993.

[56] M.Nitzberg, T.Shiota, *Non-linear image filtering with edge and corner enhancement*, IEE Trans. Imag. Process, vol. 14, pp. 826-833, Aug. 1992.

[57] S.J.Osher, J.A.Sethian *Front propagation with curvature dependent speed: Algorithms based on Hamilton-Jacobi formulations*. Journal of Computational Physics 79, pg. 12-49, 1988.

[58] N. Paragios, R. Deriche. *Geodesic Active Contours for Supervised Texture Segmentation*. Proc. of Computer Vision and Pattern Recognition 2,422-427, 1999.

[59] N.Paragios, O.Mellina-Gottardo and V.Ramesh. *Gradient Vector Flow Fast Geodesic Active Contours*, IEEE Int. Con. Comp. Vision, vol I, Jul. 01, Vancouver, Canada.

[60] P. Perona, J. Malik, *Scale space and edge detection using anisotropic diffusion*, Proc. IEEE Comp. Soc. Workshop on Comp. Vision, IEEE Computer Society Press, pp. 16-22, 1987.

[61] W. Rudin. *Complex and Real Analysis*. McGraw-Hill, Inc.

[62] L.Rudin, S.Osher, E.Fatemi. *Nonlinear total variation based noise removal algorithms*, Physica D. vol. 60, 1992.

[63] *Geometric Partial Differential Equations and image analysis* Cambridge University Press, Cambridge, U.K.,2001.

[64] G. Sapiro, B.B. Kimia, R. Kimmel, D. Shaked, A. Bruckstein. *Implementing continuous-scale morphology*. Pattern Recognition, vol. 26(9), 1992.

[65] J.A. Sethian, *Level Set Methods: Evolving Interfaces in Geometry, Fluid Mechanics, Computer Vision and Material Sciences*. Cambridge Universirty Press, Cambridge, U.K,1996

[66] K. Siddiqi, A. Tannenbaum, S.W. Zucker. *A Hanmiltonian Aaproach to the Eikonal Equation*, EMMCVPR'99, Lecture Notes in comp. Science, 1654.

[67] M. Spivak. *A Comprehensive Introduction to Differential Geometry*. Houston: Publish or Perish, cop. 1979.

[68] Ch.Sun, S. Pallotino, *Circular shortest path on regular grids*, Asian Conference on Computer Vision, pp. 852-857, Melbourne, Australia, Jan. 2002.

[69] Z.S.G. Tari, J. Shah, H. Pien. *Extraction of shape skeletons from grayscale images*. Comp. Vision and Image Understanding, vol. 66, pp. 133-146, May 1997.

[70] J.F. Traub. *Iterative methods for the solution of equations*, Prentice-Hall, Englewoods Cliffs,NJ, 1964.

[71] A.Tveito, R.Winther. *Introduction to Partial Differential Equations*, Texts in Appl. Math.

[72] J.Weickert, *Anisotropic Diffusion in image Processing*, PhD Thesis, Jan. 1996.

[73] J.Weickert, B.M. ter Haar Romeny, M.A. Viergever, *Efficient and reliable schemes for nonlinear diffusion filtering*, IEEE Trans. Im. Proc., 1998.

[74] J. Weickert, *A Review of Nonlinear Diffusion Filtering*. B. Haar Romery, l. Florack, J. Koenderink, M. Viergever (Eds.), Scale-Space Theory in Computer Vision, Lecture Notes in Computer Science, vol. 1252, Springer-Verlag, Berlin, pp. 3-28, 1997.

[75] C.Xu and J.L. Prince *Snakes, shapes and gradient vector flow*. IEEE Trans. on Image Proc., vol. 7(3), pp. 359-369, March 1998.

[76] C.Xu and J.L. Prince *Gradient Vector Flow Deformable Models*. Handbook of Medical Imaging, Isaac Bankman, Academic Press, September 2000.

[77] C.Xu and J.L. Prince *Generalized gradient vector flow external forces for active contours*. Signal Process., An Int. Journal, 71(2), pp. 132-139, 1998.

[78] C. Xu, A. Yezzi, and J. Prince, *On the Relationship between Parametric and Geometric Active Contours*. Proc. of 34th Asilomar Conference on Signals, Systems and Computers, pp. 483-489, October, 2000.

[79] G. Unal, H. Krim, A. Yezzi. *Stochastic Differential Equations and Geometric Flows*, IEEE Trans. Image Proc., vol. 11 (12), Dec. 2002.

[80] Y.-L.You, M.Ka veh, *Formation of step images during anisotropic diffusion*,Proc. ICIP '97.

[81] Y.-L.You, W.Xu, A.Tannenbaum, M.Ka veh, *Behavioral analysis of anisotropic diffusion in image processing*, IEEE Trans. Im. Proc., Nov. 1996.

[82] D. Zhang, M. Herbert, *Harmonic shape images: a representation for 3-d free-form surfaces based on energy minimization*, EMMCVPR'99, Lect. Notes in Comp. Science, 1654.

Publications

2004

- Debora Gil, Petia Radeva, "Extending Anisotropic Operators to Recover Smooth Shapes", under second revision in Computer Vision and Image Understanding.
- Debora Gil, Petia Radeva, "Inhibition of False LandMarks", submitted to ICPR'04.
- Debora Gil, Petia Radeva, "A Regularized curvature flow designed for a Selective Shape Restoration', to be published in IEEE Trans. Image Processing.

2003

- Debora Gil, Petia Radeva, "Shape Restoration via a Regularized Curvature Flow", to be published in Journal of Mathematical Imaging and Vision.
- Oriol Pujol, Debora Gil, JJ. Villanueva, Petia Radeva, "Fundamentals of Stop and Go Active Models", submitted to Imaging and Computing Vision in August 03.
- O.Rodriguez Leor, J. Mauri, E. Fernandez-Nofrerias, C. Garcia Garcia, R. Villuendas, V. Valle Tudela, D. Gil, P. Radeva, 'Reconstruction of a spatio-temporal model of the intima layer from intravascular ultrasound sequences', European Heart Journal, ESC Congress 2003, Vienna, Austria, 2003.
- Debora Gil, Petia Radeva, "Curvature vector flow to assure convergent deformable models", EMMCVPR '03, Lect. Notes in Comp. Science, vol. 2683.
- Debora Gil, Petia Radeva, Fernando Vilario, "Anisotropic Contour Completion", ICIP'03 Proceedings.
- Debora Gil, "Curvature based Distance Maps", CVC Tech. Report, n 70. Computer Science Dep., April 03.

2002

- Debora Gil, Petia Radeva, "IVUS segmentation via a regularized curvature flow". CASEIB'02 Proceedings.

- Debora Gil, Petia Radeva, Oriol Rodriguez et al. "Reconstruccin de un modelo espacio-temporal de la luz del vaso a partir de secuencias de ecografia intracoronaria.", Revista de la Sociedad Espaola de Cardiologa, vol 55 (supl2), pag 12.

- Debora Gil, "Regularized Curvature Flow". CVC Tech. Report, n 63. Computer Science Dep., Nov. 02.

- Debora Gil, Petia Radeva, Fina Mauri et al. : "Ecografia intracoronria: segmentaci automtica de l'rea de la llum", revista de la Societat Catalana de Cardiologia, Vol 4, n 4, March 02

2000

- Debora Gil, Petia Radeva, Jordi Saludes, "Segmentation of artery wall in coronary IVUS images: a probabilistic approach". IEEE Proceedings of Computers in Cardiology, 00.

- Debora Gil, Petia Radeva, Jordi Saludes, "Segmentation of artery wall in coronary IVUS images: a probabilistic approach". IEEE Proceedings of ICPR' 00.

- Debora Gil, Petia Radeva, Fina Mauri et al, "Moviment del vas en l'analisi d'imatges de ecografia intracoronria: un model matemtic", revista de la Societat Catalana de Cardiologia, Vol 3, n8, June 00.

- Fina Mauri, E.F. Nofreras, J.Comin, B.Garcia, E.Irculis, J.A.Gmez, P.Valdovinos, F.Jara, A.Cequier, E.Esplugas, O.Pujol, C.Caero, Debora Gil, P.Radeva, R.Toledo, JJ.Villanueva, "Avaluaci del Conjunt Stent/Artria mitjanant ecografia intracoronria: l'entorn informtic ", revista de la Societat Catalana de Cardiologia, Vol 3, n8, June 00.

- Debora Gil, "Complex Nilmanifolds without non-constant holomorphic functions". Prepublications of the Univ. Autnoma de Barcelona, vol. 03/2000. Mathematics Dep, Febr. 2000.

- Debora Gil, "Complex Nilmanifolds without non-constant holomorphic functions". Prepublicacions of the European Net TMR (ERB FMRX-CT96 0040). Febr. 00.